KONG XIANG-RU

"Magnetotelluric Sounding with Pulsations near Göttingen"

1. Location and instruments of observation.

In September and October 1981 field observations have been carried out near Deppoldshausen, a few kilometers northeast of Göttingen. The instruments were located on triassic Muschelkalk. Pulsations of the magnetic and telluric field were recorded digitally at two seconds sample interval, using 3-component WATERMANN induction coil magnetometers and FILLOUX-HEMPFLING electrodes (Ag-AgCl electrode in KCl solution), 200 m apart.

2. Analysis of the data

For analysis 43 record sections were selected. They were 5 to 30 minutes long and contained pronounced pulsations. The period range of analysis was 10 to 600 seconds with smooth spectral estimates at 17 periods in this interval (see Table 1 in Fig.2). Linear trends were removed, and after an harmonic analysis FOURIER-products of individual data section were smoothed with PARZEN spectral windows.

Firstly, transfer functions between the telluric field components E_n and E_e and the magnetic field components H and D were calculated by bivariate spectral analysis. They constitute the components of the impedance tensor $\underline{Z}$. Then the penetration depth z^* and the apparent resistivity ρ^* were calculated for each period from the off-diagonal elements Z_{xy} and Z_{yx} according to the definitions ($Z = Z_{xy}$ or Z_{yx})

$$z^* = \mathrm{Re}(Z/i\omega)$$

$$\rho^* = \begin{cases} 2\rho_a \cos^2\phi & \phi > 45^\circ \\ \frac{1}{2}\rho_a/\sin^2\phi & \phi < 45^\circ \end{cases}$$

with $\rho_a = \mu_o/\omega \cdot |Z|^2$ and $\phi = \arg(Z)$. No rotation of coordinates has been made, i.e. x is toward magnetic north.

For $\phi > 45^\circ$ ρ^* is the resistivity of a uniform halfspace beneath a thin well conducting top layer of conductance $\tau = (h-g)/\rho_a$, $Z/i\omega = g-ih$. For $\phi < 45^\circ$ ρ^* is the resistivity of a uniform halfspace beneath a non-conducting top layer of thickness $H = g-h$.

3. Discussion of results

The distribution of apparent resistivity ρ^* with depth z^* is plotted in Fig.1 for both off-diagonal elements separately. Both apparent resistivity plots show a smooth decrease of resistivity with depth, from a penetration depth of 3 km at 10 seconds period to about 30 km at 600 seconds. The elements Z_{xy} and Z_{yx} give similar values for z^* at all periods, but different ρ^* values, those for Z_{xy} being larger by a factor of 3.

The ρ^*-values for both elements show a slight minimum at 11 to 13 km depth z^*. Above this minimum apparent resistivities range from more than 100 Ohm · m (Z_{xy}) to about 60 Ohm · m (Z_{yx}). Below they converge to about 40 Ohm · m. This appears to be the mean upper mantle resistivity beneath the recording site.

The values of skewness S and anisotropy A are shown in Fig.2. Both parameters do not change with period in any systematic way. S is quite small (0.2) and thus 3-D effects appear to be unimportant at the point of observations. The parameter A deviates consistently and significantly from unity. So a 2-D structure affects the impedance, but no inference can be made about its strike or cause. The anisotropy of the impedance of pulsation is consisting with results from the analysis of Sq which shows that $|Z_{yx}|$ is smaller and $|Z_{xy}|$ is greater than the normal part of Z.

Telluric vectors are illustrated in Fig.3. For magnetic polarisation in east direction the telluric vectors $\underline{e}_y$ consistently deviate from their undisturbed north direction by about 20° toward west. The deflection of the telluric vectors $\underline{e}_x$ from their normal west direction is somewhat smaller and increases with period. In either case the distortion of the telluric field is obvious, but similar for the in-phase and out-of-phase current and not very different from that found for bays and diurnal variations. So the distortion appears as quasi-static and its cause should be local.

4. Model calculations

The results of model calculations, using the ψ-algorithmus to interpret the logarithmic response$\{\ln \rho_a/\rho_o + 2i(\pi/4 - \phi)\}$, are shown in Fig.4 and 5. As was to be expected from the $\rho^*(z^*)$ plots, the results of 3-layer models agree essentially with the observational results. The rms fit ε for the logarithmic response is 0.187 for Z_{yx} and 0.138 for Z_{xy}, i.e. the apparent resistivity ρ_a is

reproduced within about 19% and 14%, respectively. From Fig.4 also can be seen the parameters of the second and third layer are similar for Z_{xy} and Z_{yx}, but not in the first layer which suggests lateral inhomogenity of this layer. In Fig.5 the interpretation of Z_{yx} by a 4-layer model is shown in an attempt to resolve the crustal conductor at intermediate depth. This is possible when some model smoothing with MARQUART's $\alpha = 0.1$ is applied. The good conductor appears now as third layer at 24-25 km depth. The half-space below, representing the upper mantle, has a resistivity of 50 to 80 Ohm·m. The resistivity of the second layer, representing the upper crust is now shifted to more than 500 Ohm · m. The top layer, 3.5 km thick and with a resistivity of 18-20 Ohm · m, represents sediments above the basement with a conductance of 170 Siemens.

By the inclusion of a fourth layer the rms fit ε is improved to 0.126. The plot of ε versus the layer parameters d_o in Fig.5 shows this value as a clear minimum. The overall fit for ρ_a is now 6.4 Ohm · m and that of the phase 2.6 degrees. The resolution is quite satisfactory as evident from the resolution matrix A in Fig.5. With respect to the very low resistivity of 1.5 Ohm · m in the third layer it should be observed that no weights were used. This means that the ratio of layer thickness to the square rost of layer resistivity is a constant for all layers.

5. Acknowledgements

I am very grateful to Prof. U. Schmucker, Dr. E. Steveling and Dr. M. Richards for their direction and help. I wish also to thank the support and help of the Geophysic Institut of Göttingen University.

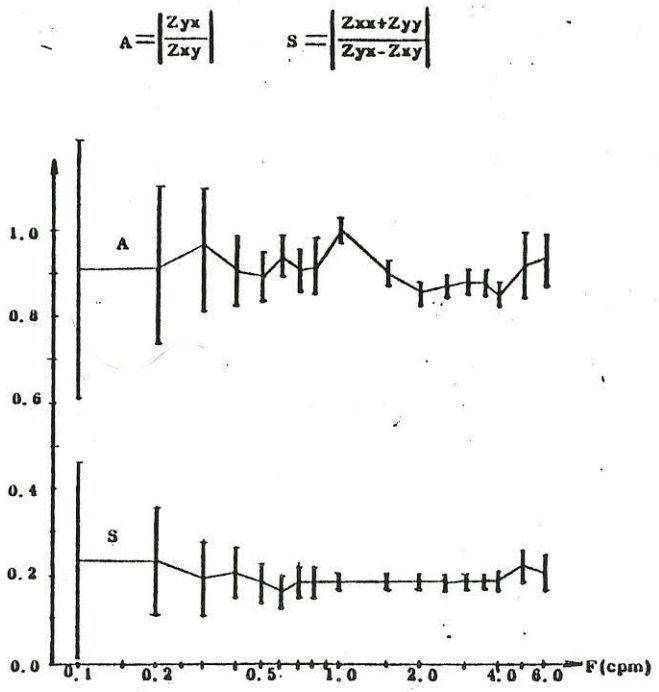

Fig.2: The values of anisotropy (A) and skewness (S).

Table 1: Period and frequency ranges of data analysis

Selected periods (s)	Frequency
600	0.1
300	0.2
200	0.3
150	0.4
120	0.5
100	0.6
85.7	0.7
75	0.8
60	1.0
40	1.5
30	2.0
24	2.5
20	3.0
17.1	3.5
15	4.0
12	5.0
10	6.0

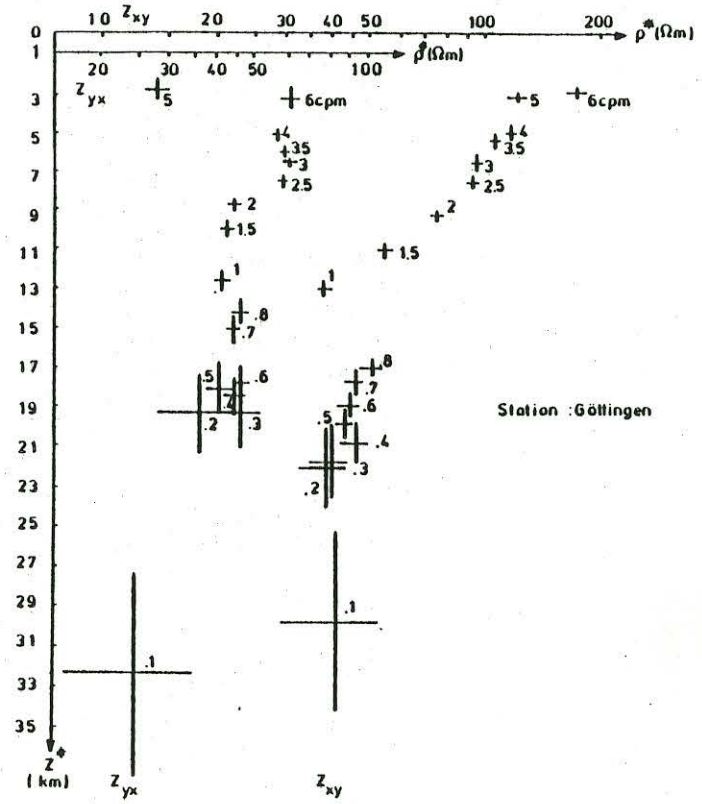

Fig.1: The distribution of apparent resistivity ρ^* with z^* .
The above abscissa use for Z_{xy} data (right).
The lower abscissa use for Z_{yx} data (left)

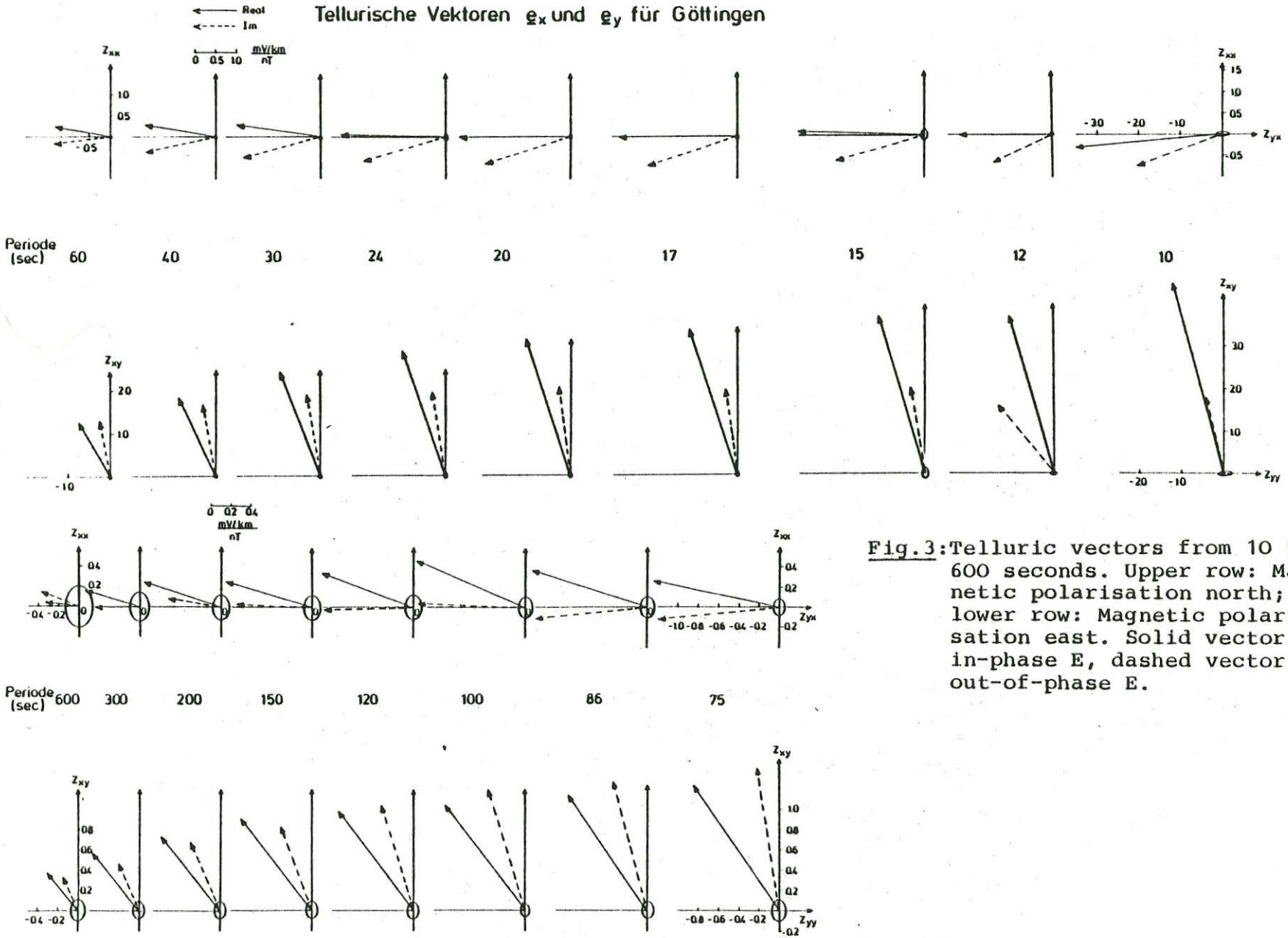

Fig.3: Telluric vectors from 10 to 600 seconds. Upper row: Magnetic polarisation north; lower row: Magnetic polarisation east. Solid vector: in-phase E, dashed vector: out-of-phase E.

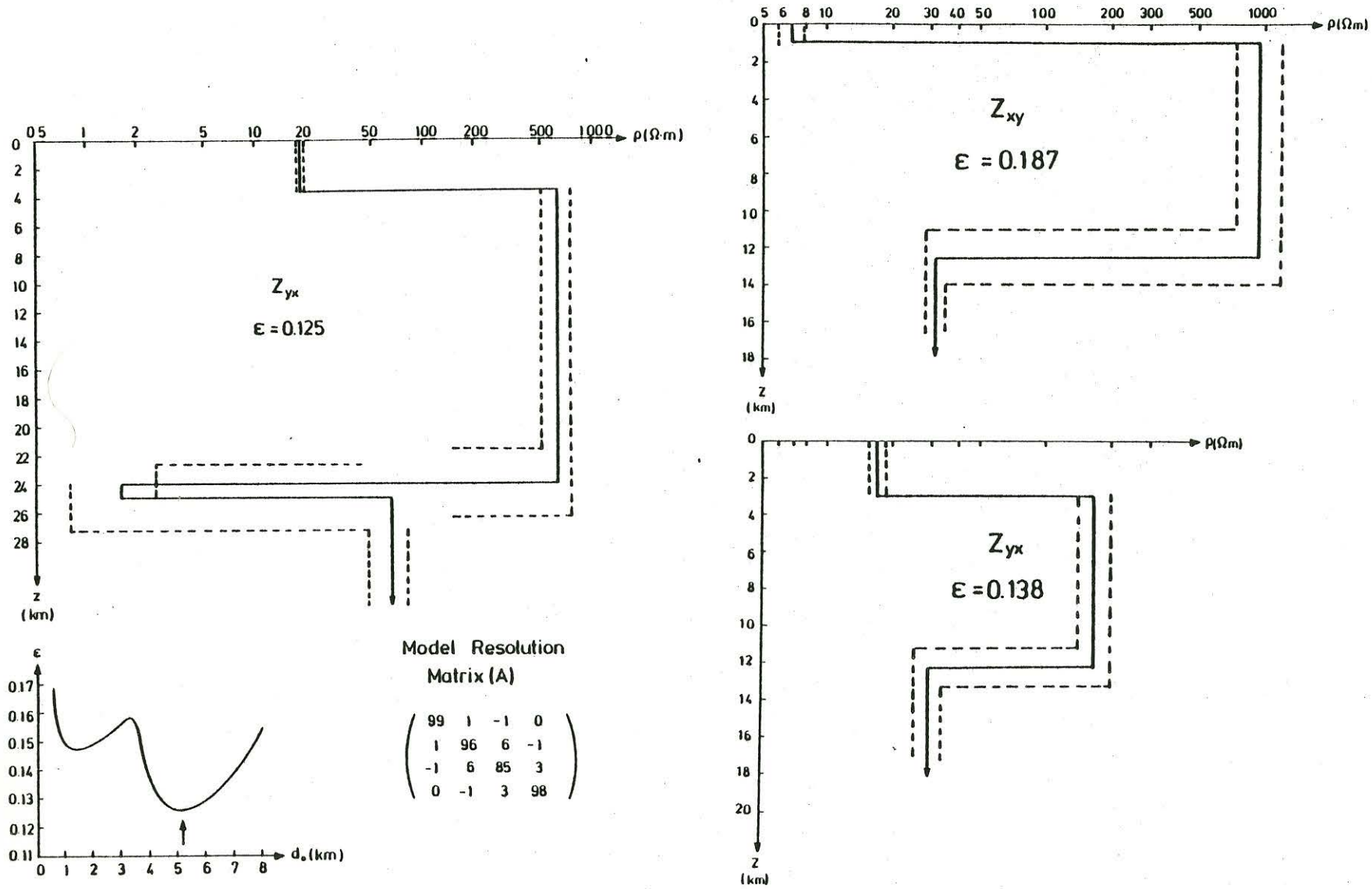

Fig.4 and 5: Three and four layer models for off-diagonal impedance tensor elements.
ε: Residual for 17 logarithmic response values.